

## SUSTAINED LOAD EFFECTS ON THE SEISMIC PERFORMANCE OF CONCRETE COLUMNS

A. E. Schultz<sup>1</sup>, S. S. Welton<sup>2</sup>, L. E. Rey<sup>3</sup>

### Abstract

An integrated experimental and analytical research program is undertaken to define the effects of sustained axial load on the seismic performance of reinforced concrete columns. Thirteen beam-column specimens are subjected to simulated seismic lateral loads after the columns sustain axial load for a predefined duration. The experiments are supplemented by computer analyses that simulate 1) redistribution of compression stress during sustained axial load periods, and 2) nonlinear flexural response to short-term lateral loads. Columns which sustained load for longer durations are observed to develop inclined cracks at earlier stages of the lateral load tests, and this damage led to 1) large decreases in lateral stiffness prior to column hinging, 2) modest decreases in peak strength, and 3) marked reductions in energy absorption.

### Introduction

During the past decade, seismic evaluation and performance of existing structures has taken an increasingly important role in the earthquake engineering community in the U.S. In this vein, the present study has as a principal objective the determination of the effects of sustained gravity loads on the seismic performance of reinforced concrete buildings. The study focuses on the effects of sustained axial load in reinforced concrete columns, as the role of columns is critical to the resistance of concrete buildings to earthquake motions.

Tests by Troxell et. al. (1958) demonstrated that sustained axial load can mobilize redistribution of axial stresses in reinforced concrete columns. In time, unrestrained concrete

---

<sup>1</sup>Research Structural Engineer, Building and Fire Research Laboratory, National Institute of Standards and Technology, Gaithersburg, MD 20899

<sup>2</sup>Structural Engineer, Stroud Pence Associates, Virginia Beach, VA 23462

<sup>3</sup>Structural Engineer, Energy Services, Brown & Root, Inc., Houston, TX 77072

undergoes creep and shrinkage deformations, while long-term deformations in steel are relatively insignificant. Compatibility of axial strain requires that concrete unload compression stress to longitudinal reinforcement. The present study addresses the effects of such stress redistributions, which are likely to have taken place in most existing concrete buildings, on column behavior during an earthquake. It is important to note that laboratory investigations on the cyclic load response of concrete structures and components are conducted when specimens are approximately one month old, and tests are completed within a few hours of initial load application. As such, laboratory investigations to date have insulated concrete specimens from long-term effects.

### Experimental Design

The present study is described in greater detail elsewhere (Rey and Schultz, 1991; Welton and Schultz, 1992). In designing the test specimens, points of inflection were assumed at mid-length of columns and beams in a laterally-loaded frame. The model was further simplified by removing the bottom column. During the lateral load tests (Fig. 1a), the specimens were supported by pins at the ends of the beams, and by a roller below the beam-column joint. A constant axial load and a short-term, cyclic lateral load history were applied to the tip of the column. Furthermore, the columns were subjected to constant axial loads for a predefined duration in sustained axial load tests conducted prior to the lateral load tests.

The experimental program is summarized in Table 1. A total of thirteen beam-column specimens, organized in three series, were fabricated and tested. Specimen 1A-2 is a replica of specimen 1A which was damaged prior to the lateral load test, and 1A-2 was cast from a different batch of concrete at a later time. Experimental variables included sustained axial load period, magnitude of axial load, and amount of column transverse reinforcement. All columns had an overall depth of 152 mm, and a 203-mm width was selected to discourage out-of-plane bending. Beam cross-sections were 203 mm wide and 254 mm deep, which forces hinging into the columns. Hot-rolled deformed reinforcing bars was used for all longitudinal reinforcement.

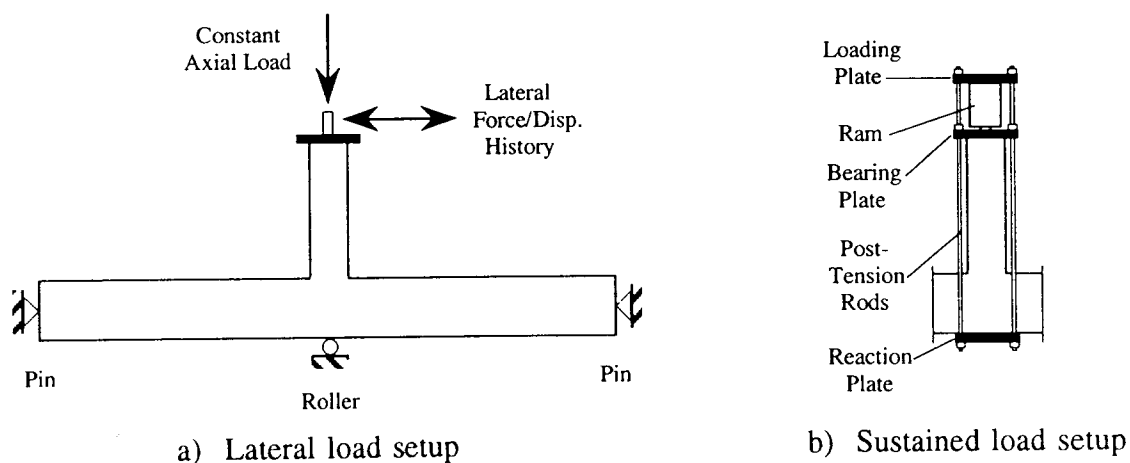


Figure 1. Test setup.

As noted in Table 1, two different column tie arrangements were selected, both which utilized single, closed, rectangular ties with 135° hooks. Transverse reinforcement for columns

in Series 1, as well as specimens 3-B and 3-D, was proportioned to meet or exceed current building code provisions for exposure to the highest seismic risk (ACI, 1989), while nominal ties were used in all other specimens (Series 2 and specimens 3A and 3C) to represent practice prior to seismic design. Due to the relative amounts of transverse reinforcement, the former are referred to as heavily-reinforced specimens and the latter as lightly-reinforced. For all beams, closed rectangular ties bent from 6.4-mm diameter cold-drawn wire were spaced at 108 mm.

Table 1. Experimental program.

Parameter	Series 1	Series 2	Series 3L	Series 3H	1A-2
<b>Material Strengths</b>					
$f'_c$ (N/mm <sup>2</sup> )	29.8	33.1	29.9	29.9	36.5
$F_y$ (N/mm <sup>2</sup> )	414	414	414	414	414
$F_{yh}$ (N/mm <sup>2</sup> )	634	476	476	634	634
<b>Reinforcement</b>					
Longitudinal	4-#4	4-#4	4-#4	4-#4	4-#4
$\rho$	1.63%	1.63%	1.63%	1.63%	1.63%
Transverse*	6.4 $\phi$ @25	4.2 $\phi$ @64	4.2 $\phi$ @64	6.4 $\phi$ @25	6.4 $\phi$ @25
$\rho_h$	3.23%	0.58%	0.58%	3.23%	3.23%
<b>Loads</b>					
Nominal Axial Load (kN)	222	222	111	111	222
Actual Sustained Load Period (days)	A/0 B/56 C/91 D/203	A/0 B/30 C/90 D/247	A/0 --- C/78 ---	--- B/0 --- D/79	0

\*Wire diameter and pitch in mm.

### Sustained Load Tests

During the sustained axial load period, the columns were loaded using a system of external post-tensioning rods and steel plates (Fig. 1b). Initial axial load was applied using a hydraulic ram, and steel nuts were used to clamp the column between steel plates and contain the axial force. Load was monitored using strain gages in the post-tensioning rods, and adjustments were made periodically by adjusting the nuts. Strains in column longitudinal bars were monitored using strain gages, and concrete strains in two opposing column faces were obtained from length changes measured between steel targets.

The 222-kN column axial load used for the specimens in series 1 and 2 represents 60% and 22%, respectively, of the nominal axial loads for balanced strain failure and pure compression failure. Column axial loads were maintained within  $\pm 4\%$  of their targeted values during the sustained load period. For specimens A, B, C and D in series 1 and 2, nominal sustained load durations of 0, 30, 90 and 240 days, respectively, were selected initially. It is expected that concrete at these ages has developed approximately 0, 50%, 75% and 90%, respectively, of total long-term deformation. There was some variation of these nominal sustained load periods as noted in Table 1.

Large long-term deformations were measured in the columns during the sustained load tests, with the final strains being four and five times larger, respectively, than the initial strains in specimens 1D and 2D. These deformations were accompanied by sizable redistribution of internal axial stresses. The axial load ratio in Table 2 indicates four-fold and six-fold increases, respectively, for the ratio of axial forces in column longitudinal steel and concrete for specimens 1D and 2D. Clearly, stress redistribution is proportional to sustained load period.

Table 2. Summary of tests.

Specimen	Load Ratio		Yield Force* (kN)	Yield Disp.* (mm)	Yield Stiffness* (kN/mm)	Concrete Stress† (N/mm <sup>2</sup> )	Cracking Load (kN)
	Init. (%)	Final (%)					
1A	14	--	31.3	11.8	2.64	6.76	34.8
1B	14	25	33.1	11.4	2.91	5.72	33.0
1C	14	41	30.1	13.2	2.28	5.03	31.9
1D	14	63	34.4	13.2	2.22	4.27	30.6
2A	11	--	29.4	9.7	3.03	6.89	37.0
2B	11	38	31.4	12.6	2.49	5.03	33.7
2C	11	52	32.3	12.9	2.50	4.62	32.9
2D	11	69	28.8	13.2	2.17	4.21	32.2
3A	13	--	26.9	9.1	2.95	3.38	29.0
3B	13	--	26.6	9.3	2.85	2.48	27.5
3C	13	58	28.2	11.7	2.42	2.41	27.4
3D	13	71	26.5	10.7	2.48	2.14	27.0
1A-2	10	--	32.6	8.8	3.70	7.03	39.1

\*Average of both loading directions.

†Measured at the beginning of the lateral load test.

## Transverse Shrinkage

An interesting observation was made during the sustained axial load tests: As the concrete in the column cores shrank, the column ties acted to restrain this transverse strain. Thus, the ties accumulated compression stress and exerted a transverse tension stress on the concrete. Column tie strains were measured during the sustained axial load tests only for specimens 3C and 3D, and the mechanism described above was clearly evident in these measurements. The interesting feature of this mechanism is that the ties were acting in compression, rather than tension, and the column with more transverse reinforcement (3D) was subjected to larger lateral tension stresses.

To investigate the mechanism of restrained transverse shrinkage described above, the computer-based analysis procedure implemented and used successfully by Rey and Schultz (1991) for analysis of axial stress redistribution was applied to the transverse direction of the column. The axial stress redistribution analysis is based on a model proposed by Samra (1982). For restrained transverse shrinkage analysis, the legs of the column ties were treated as the restraining reinforcement, and shrinkage strains in the concrete became the forcing function for redistribution of internal stresses in the transverse direction of the column.

Extensive parametric study of this phenomenon was conducted to gain a better understanding of the magnitude of this mechanism. Over a wide variation in concrete material properties and column tie reinforcement, transverse tension stresses ranging from 0.034 to 1.38 N/mm<sup>2</sup> were computed for columns similar to those in this study. The impact of these tension stresses was evaluated using a confinement model for concrete columns proposed by Saatcioglu and Razvi (1992) and which is based on the concept of effective lateral pressure. The transverse tension stresses were treated as negative lateral pressures, and confined compression strengths were calculated in the axial direction of the columns.

While decreases in confined compression strength were obtained, calculated confined compression strengths  $f'_{cc}$  always exceeded unconfined compression strength  $f'_c$ . The detrimental effects of shrinkage-induced transverse tension stresses are offset by a number of factors. First, creep serves to relax any restrained shrinkage effect. Second, the large magnitude of strength enhancement afforded by lateral confinement overshadows transverse tension stresses, particularly for cases in which lateral pressures are low. Third, concrete strength gain with time is of the same order of magnitude as the reductions afforded by restrained transverse tension stress.

## Lateral Load Tests

All specimens were subjected to the same short-term lateral displacement history. Lateral load/displacement was applied by a servo-controlled hydraulic actuator, and column axial load was applied by a hydraulic ram through a device that enabled lateral displacement of the column tip. This device comprised a large structural steel tube with ball-socket joints at both ends and a group of three stiff linear springs. The springs introduced flexibility to the axial degree-of-freedom of the concrete column which would otherwise have a very large stiffness. This device was adapted from an experimental investigation by Low and Moehle (1987).

The lateral displacement history comprised symmetric cycles of reversing column tip displacements, with the peak displacement during the first two full cycles being equal to the yield displacement. Peak amplitude of each subsequent pair of cycles was augmented by one-half of the nominal yield displacement. Loads, displacements and strains were sampled, conditioned and stored by a microcomputer-controlled data acquisition system at each load step. Approximately forty load steps were used to define each full cycle of the displacement history. Typical force-displacement curves are shown in Fig. 2 for lightly-reinforced specimens 3A and 3C, and Table 2 summarizes some pertinent results from these tests.

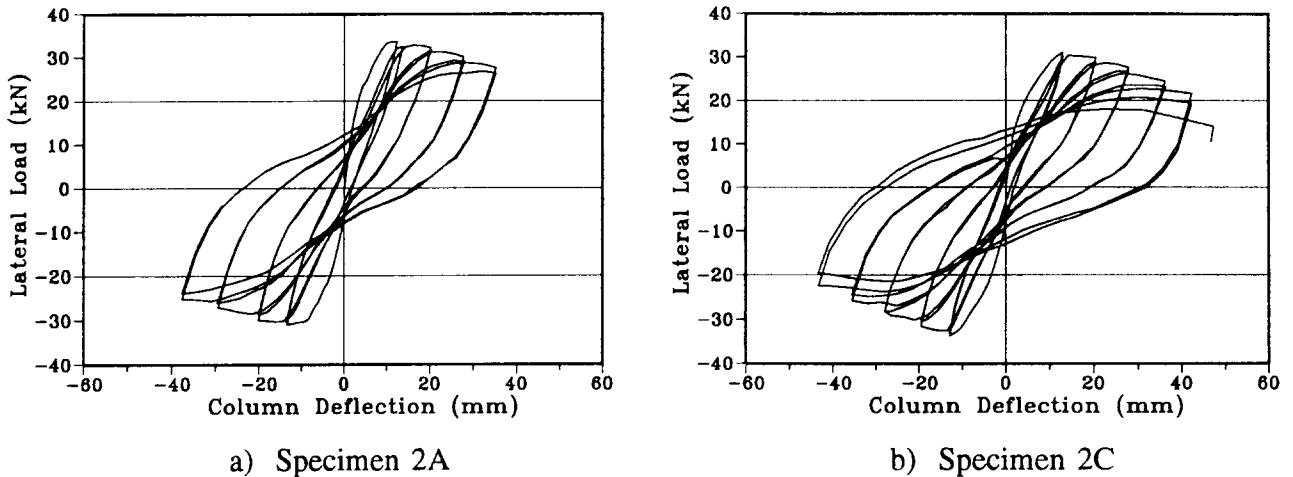


Figure 2. Force-displacement hysteresis curves.

None of the specimens failed by losing all load-carrying capacity in a sudden manner. Rather, cumulative damage from load reversals led to the eventual loss of a large fraction of strength. During the lateral load tests, all specimens exhibited strength and stiffness deterioration, as well as pinching of the force-displacement relations. These features became more pronounced in specimens with long sustained load durations and small amounts of transverse steel.

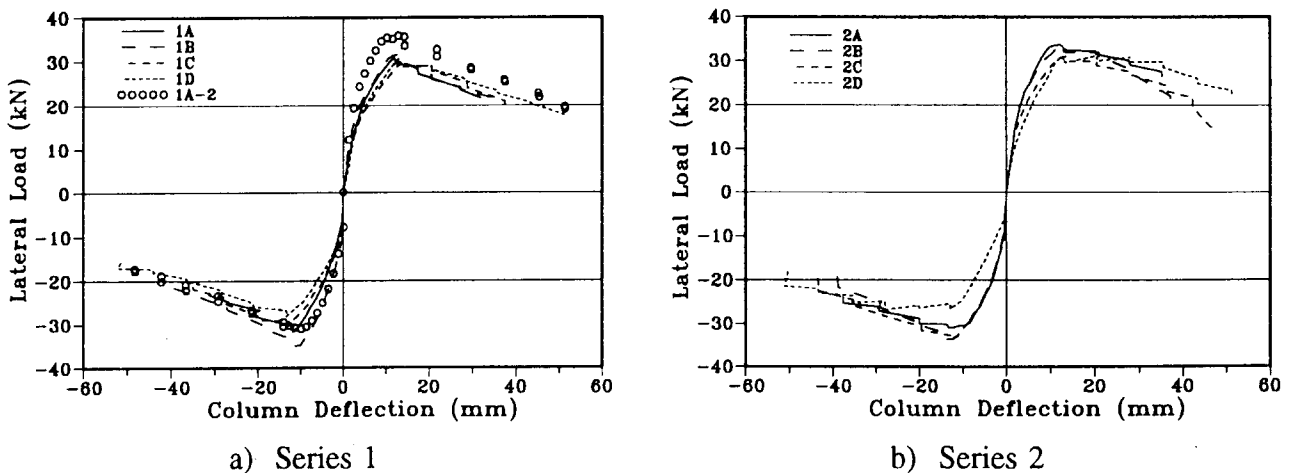


Figure 3. Force-displacement envelopes.

Force displacement envelopes are shown in Fig. 3 for all specimens in series 1 and 2. Modest reductions in peak strength can be observed for specimens with larger sustained load period. The only exception is specimen 1A, but it is noted that specimen 1A-2 displayed larger peak force than any specimen in series 1. The envelopes in Fig. 3 also illustrate measurable decreases in column stiffness prior to first yielding, and, this stiffness consistently decreases for columns with larger sustained load periods. Effective yield stiffnesses, defined as the ratio of force at first yield to displacement at first yield, is given in Table 2. Differences as large as 40% (1D vs. 1A-2) and 30% (2D vs. 2A) appear to be attributed to long-term effects. Force-displacement envelopes calculated using a modified version of the fiber model proposed by Poston (1982) agree with the initial portion of the ascending branch of the measured envelopes, but the computational procedure was unable to simulate the inclined cracking of the columns. This phenomenon which is discussed in the next section dominated column behavior.

The capacity of the columns to dissipate energy by hysteresis was also undermined by the internal stress changes incurred during the sustained axial load tests. The cumulative area enclosed by force-displacement hysteresis loops was normalized by the product of yield force and yield displacement (Table 2) to define the energy dissipation factor (EDF). The normalization allows comparison among specimens with differing strength and stiffnesses, and it also serves as a vehicle to correlate energy absorbed by hysteretic behavior to equivalent viscous damping. Energy dissipation factors at the end of the 8th full cycle of load (i.e. the second full cycle at a displacement ductility equal to 2.5) are shown in Fig. 4 against concrete compression stress measured at the beginning of the short-term lateral load tests.

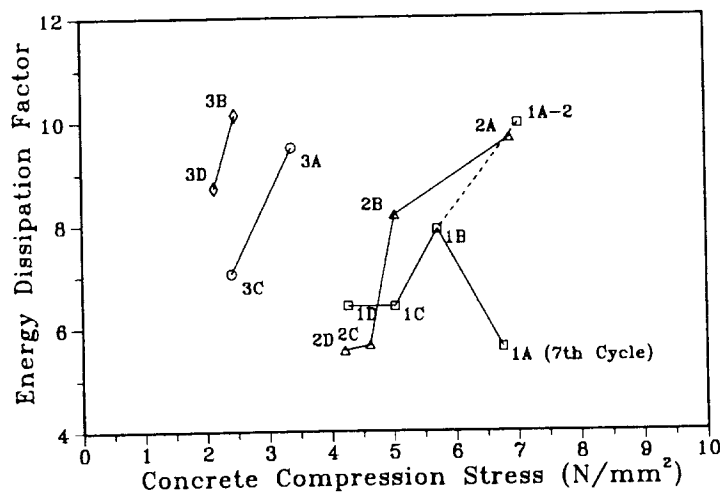


Figure 4. Energy dissipation factor after 8 cycles of load.

A basic trend is clearly evident in Fig. 4 among all three series of specimens: As concrete compression stress decreases with increased duration of sustained axial load, EDF decreases. Reductions in EDF as large as 40% are noted for series 2, and the apparent rate of change in EDF with concrete compression stress is larger for the lightly-reinforced specimens (series 2 and specimens 3A and 3C). It is also worth noting that approximately one-half of the observed decreases in EDF are a direct result of reduced areas in the force-displacement hysteresis loops, and the remainder is due to increases in yield displacement.

## Diagonal Cracking

During the lateral load tests, inclined cracks were observed to form at the base of the columns. It was further observed that these cracks initiated and propagated at lower lateral loads in specimens that sustained axial loads for longer durations. According to the shear provisions in the ACI 318-89 document (ACI, 1992), the nominal shear stress  $v_c$  at diagonal cracking (in  $\text{N/mm}^2$ ) for a flexural member which is subjected to axial compression is given by

$$v_c = 0.166 \left( 1 + 0.0725 \frac{N_u}{A_g} \right) \sqrt{f'_c} \quad (1)$$

where  $f'_c$  is concrete compression strength in  $\text{N/mm}^2$ ,  $N_u$  is axial compression force in N, and  $A_g$  is gross area of the column cross-section in  $\text{mm}^2$ .

Cracking strengths were estimated using Equation 1, but the ratio  $N_u/A_g$  was replaced with measured concrete compression stress in each column at the beginning of the lateral load test, and nominal stress  $v_c$  was multiplied by column width  $b$  and effective depth  $d$ . The estimated cracking strengths are listed in Table 2 along with the concrete compression stresses.

The estimated cracking shear strengths in Table 2 indicate that as much as a 12% decrease in cracking shear force can be expected with the reductions in concrete compression stresses noted between the A and D specimens in both series 1 and 2. It is equally interesting to note that the estimated cracking shear forces are larger than the measured yield forces in every case, yet every single specimen developed inclined cracks at lateral loads that are smaller than the estimated diagonal cracking strength. Damage to concrete with cyclic loading appears to be responsible for this discrepancy, as Equation 1 was developed for monotonic loading, and each specimen underwent several complete load cycles before developing inclined cracks.

The mechanism of inclined cracking described above appears to be responsible for the observed differences in behavior of the column specimens during the lateral load tests. Premature inclined cracking during lateral loading was mobilized by the reduction in concrete compression stress associated with internal stress redistribution during the sustained axial load tests. Subsequently, the premature inclined cracks accelerated the deterioration of column strength and stiffness, and these changes in the resistance characteristics of the column distorted the shape of the force-displacement hysteresis loops which resulted in decreased energy dissipation capacity.

## Conclusions

Axial load sustained over a long period of time can have detrimental effects on the response of concrete columns to short-term lateral loads. Sustained load effects were observed to reduce column strength by no more than 10%, but pre-yield stiffness for the specimens with longest sustained load duration (1D and 2D) displayed stiffness reductions on the order of 30-40%. Energy dissipation capacity was also observed to decrease by as much as 40% with long-duration sustained loads. Increasing the amount of column tie steel reduced sustained load effects, but even large transverse reinforcement ratios did not fully eliminate them. Also,

restrained shrinkage was observed to generate transverse tension stresses in the column core, but it was determined that these stresses do not have a measurable effect on column strength.

The primary mechanism responsible for the observed changes in the resistance characteristics of the columns is the reduction in concrete axial compression stress, which is mobilized by axial stress redistribution resulting from long-term concrete deformations. As axial compression stress in the concrete decreases with sustained load duration, the lateral load at which the column develops inclined cracks is suppressed. This reduction in cracking strength leads to accelerated deterioration of the column upon application of short-term lateral loads.

### Acknowledgements

This research was conducted with financial support from the National Science Foundation under grant CES-8809320 with A. J. Eggenberger and Henry J. Lagorio as Program Directors. This support is gratefully acknowledged. The work was completed while the first author was Faculty Member and the second and third authors were Graduate Research Assistants in the Department of Civil Engineering at North Carolina State University.

### References

- American Concrete Institute. "Building Code Requirements for Reinforced Concrete." Detroit, MI, 1989.
- Low, S. S. and J. P. Moehle. "Experimental Study of Reinforced Concrete Columns Subjected to Multi-Axial Cyclic Loading." Report No. UCB/EERC-87/14. Earthquake Engineering Research Center. University of California, Berkeley, September, 1987.
- Poston, R. "Computer Analysis of Slender Nonprismatic or Hollow Bridge Piers," M.S. diss., The University of Texas, Austin, 1980.
- Rey, L. E. and A. E. Schultz. "Effects of Sustained Axial Load on the Behavior of Reinforced Concrete Columns: Part 1 - Analysis." Department of Civil Engineering. North Carolina State University, Raleigh, January 1991.
- Saatcioglu, M. and S. R. Razvi. "Strength and Ductility of Confined Concrete." ASCE Journal of Structural Engineering 118, no. 6 (June 1992): 1590-1607.
- Samra, R. M. "Time-Dependent Deformations of Reinforced Concrete Columns," Ph.D. diss., University of Illinois, Urbana, 1982.
- Troxell, G. E., Raphael, J. M., and R. E. Davis. "Long-Time Creep and Shrinkage Tests of Plain and Reinforced Concrete." Proceedings, ASTM 58 (1958): 1101-1120.
- Welton, S. S. and A. E. Schultz. "Effects of Sustained Axial Load on the Behavior of Reinforced Concrete Columns: Part 2 - Experiment." Department of Civil Engineering. North Carolina State University, Raleigh, June 1992.

The Earthquake Engineering Research Institute (EERI), the Organizing Committee, and the financial sponsors of the Fifth U.S. National Conference on Earthquake Engineering assume no responsibility for the statements made in the papers of these proceedings; any opinions expressed are those of the individual authors. Interested readers should contact the individual authors for necessary clarification.

The material contained herein reflects reproduction and reduction from original materials submitted by the individual authors. The variable quality of the copy is unavoidable due to the scope of the project.

*Cover design:* Mahjoub Elnimeiri and Jamshid Mohammadi

*Cover graphics:* Andrew M. Neu and David M. Ozouf

*Production Coordinator:* Frances M. Christie

*Production Assistance:* Star Type, Berkeley, California  
Wendy Warren

© 1994 by Earthquake Engineering Research Institute  
499 14th Street, Suite 320  
Oakland, California 94612-1902  
(510) 451-0905 Fax (510) 451-541

Copies of these proceedings may be obtained directly from EERI.

*All rights reserved.* No part of this book may be reproduced, in any form or by any means, without permission in writing from the Earthquake Engineering Research Institute.

*Printed in the United States of America*

ISBN 0-943198-46-1

 Printed on Recycled Paper